Synthesis, Properties, and Characterization of Nanometer-Size Metal Particles by Homogeneous Reduction with Alkalides and Electrides in Aprotic Solvents

Kuo-Lih Tsai and James L. Dye*

Department of Chemistry and Center for Fundamental Materials Research, Michigan State University, East Lansing, Michigan 48824

Received December 8, 1992. Revised Manuscript Received February 1, 1993

A new method for the preparation of small metal/oxidized metal particles is described that utilizes homogeneous reduction of metal salts by dissolved alkalides or electrides in an aprotic solvent such as dimethyl ether or tetrahydrofuran. Soluble compounds of transition metals and post-transition metals in dimethyl ether or tetrahydrofuran were rapidly reduced at −50 °C by dissolved alkalides or electrides to produce metal particles with crystallite sizes from <3 to 15 nm. The products were characterized by X-ray photoelectron spectroscopy. Confirmation by electron diffraction was made in the case of air-stable samples. The average particle size was estimated from powder X-ray diffraction line broadening. Particle size distributions were determined by counting the particles on electron micrographs obtained by transmission electron microscopy. Salts of Au, Cu, Te, and Pt formed metallic particles with little or no oxidation even when washed with degassed methanol. Reduction of salts of Ni, Zn, Ga, Mo, Sn, and Sb yielded surface oxidation over a metallic core. Stoichiometric amounts of the alkalide or electride were used; these were prepared either separately or in situ. FT-IR spectroscopy was used to demonstrate the presence of organic decomposition products on the surface of the metal particles. This method is also applicable to the formation of finely divided metals on oxide supports.

Introduction

The preparation of nanoscale particles (1–20-nm diameter) as colloids or aggregates is a well-developed field that involves a variety of chemical and physical techniques.[1,2] Small noble-metal particles are commonly made by mild reduction.[3–5] Rieke and co-workers and others have reduced salts of the more active metals in ethereal or hydrocarbon solvents, either heterogeneously with alkali metals (slow) or homogeneously with radical anions of aromatic compounds such as naphthalene (fast).[6–10] The products of such reactions are highly active metal powders. Other methods such as pyrolysis of precursors,[11] evaporation of metals,[12] matrix isolation (solvated metal atom dispersion),[13,14] and sol–gel processes[15] have also been used to prepare small metal particles. Two more recent developments are reduction with alkali-metal organoborohydride solutions, such as $NaB(Et)_3H$, that has been shown to yield both single metals and alloys of the iron-group elements and the noble metals[16] and reduction with BH_4^- for Co, Ni, Au, Ag, Pt, etc.[17]

Alkalides and electrides are crystalline ionic salts that contain either alkali-metal anions or trapped electrons. These compounds crystallize from solution to yield shiny bronze-colored crystals (alkalides) or black crystals (electrides) which are all reactive toward air and moisture and are thermally unstable at room temperature. Because of their unusual nature and properties, they have been studied by a variety of experimental methods. These include optical studies,[18] nuclear magnetic resonance spectroscopy,[19] electron paramagnetic resonance spectroscopy,[20] luminescence spectroscopy,[21] magnetic susceptibility,[22] single-crystal X-ray crystallography,[23] powder X-ray diffraction,[24] photoemission spectroscopy,[25] and pressed powder electrical conductivity.[26,27]

Because alkalides and electrides are air sensitive and thermally unstable, their synthesis must be done at low

(1) Fievet, F.; Lagier, J. P.; Figlarz, M. *MRS Bull.* **1989**, *14* (12), 29.
(2) Livage, J.; Henry, M.; Jolivet, J. P.; Sanchez, C. *MRS Bull.* **1990**, *15* (1), 18.
(3) Schloten, J. J. K.; Konvalinka, J. A.; Beekman, F. W. *J. Catal.* **1973**, *28*, 209.
(4) Wilenzick, R. M.; Russel, D. C.; Morris, R. H.; Marschall, S. W. *J. Chem. Phys.* **1967**, *47*, 533.
(5) MacKee, D. W.; Norton, F. J. *J. Phys. Chem.* **1964**, *68*, 481.
(6) Rieke, R. D. *Science* **1989**, *246*, 1260.
(7) Chao, L.; Rieke, R. D. *J. Organomet. Chem.* **1974**, *67*, C64.
(8) Rieke, R. D.; Bales, S. E. *J. Am. Chem. Soc.* **1974**, *96*, 1775.
(9) Rieke, R. D.; Hudnall, P. M. *J. Am. Chem. Soc.* **1972**, *94*, 7178.
(10) McCormick, M. J.; Moon, K. B.; Jones, S. R.; Hanusa, T. P. *J. Chem. Soc., Chem. Commun.* **1990**, 778.
(11) Fox, P. G.; Ehretsman, J.; Brown, C. E. *J. Catal.* **1971**, *20*, 67.
(12) Philips, W. B.; Desloge, E. A.; Skofronick, J. G. *Appl. Phys.* **1967**, *39*, 3210.
(13) Klabunde, K. J.; Hfner, H. F.; Murdock, T. O.; Ropple, R. *J. Am. Chem. Soc.* **1976**, *98*, 1021.
(14) Klabunde, K. J.; Li, Y. X.; Tan, B. *Chem. Mater.* **1991**, *3*, 30.
(15) Jean, J. H.; Ring, T. A. *Langmuir* **1986**, *21*, 251.
(16) Bonnemann, H.; Brijoux, W.; Joussen, T. *Angew. Chem., Int. Ed. Engl.* **1990**, *29*, 273.
(17) Glavee, G. N.; Klabunde, K. J.; Sorenson, C. M.; Hadjipanayis, G. C. *Langmuir* **1992**, *8*, 771 and references therein.
(18) Dye, J. L. *Angew. Chem., Int. Ed. Eng.* **1979**, 18, 587.
(19) Dye, J. L.; Andrews, C. W.; Ceraso, J. M. *J. Phys. Chem.* **1975**, *79*, 3076.
(20) Ellaboudy, A. E.; Bender, C. J.; Kim, J.; Shin, D. H.; Kuchenmeister, M. E.; Babcock, C. T.; Dye, J. L. *J. Am. Chem. Soc.* **1991**, *113*, 2347.
(21) Bannwart, R. S.; Solin, S. A.; DeBacker, M. G.; Dye, J. L. *J. Am. Chem. Soc.* **1989**, *111*, 5552.
(22) Issa, D.; Ellaboudy, A. E.; Janakiraman, R.; Dye, J. L. *J. Phys. Chem.* **1984**, *88*, 3847.
(23) Dawes, S. B.; Ward, D. L.; Huang, R. H.; Dye, J. L. *J. Am. Chem. Soc.* **1986**, 108, 3534.
(24) Doeuff, S.; Tsai, K. L.; Dye, J. L. *Inorg. Chem.* **1991**, *30*, 849.
(25) Huang, R. H. Ph.D. Dissertation, Michigan State University, 1987.
(26) Papaioannou, J.; Jaenicke, S.; Dye, J. L. *J. Solid State Chem.* **1987**, *67*, 122.
(27) Moeggenborg, K. J.; Papaioannou, J.; Dye, J. L. *Chem. Mater.* **1991**, *3*, 514.

0897-4756/93/2805-0540$04.00/0

temperatures in the absence of air, moisture, and other reducible substances. The synthesis of alkalides and electrides via vacuum line techniques has been described in detail elsewhere.[28,29]

Alkalides and electrides form M^- and e^-_{solv} when dissolved in a nonreducible solvent. These species are the strongest reducing agents that can exist in solution. Preliminary experiments that resulted in the formation of small metal particles (<3–15-nm diameter) of a wide range of transition metals and post-transition metals were previously described in a brief publication.[30] In this paper, we discuss in greater detail the synthesis, properties, and characterization of these metal particles.

Experimental Section

The aprotic solvents Me_2O or THF were distilled from solutions of excess Na–K and benzophenone into stainless steel (Me_2O) or glass (THF) storage vessels. Liquid 15-crown-5 was purified by distillation. All the alkali metals and metal salts were purchased from Aldrich or AESAR in the highest available purity without any further purification. Liquid samples were $TiCl_4$ (99.995+%), $SbCl_5$ (99%), and $SnCl_4$ (99.999%). Solid samples were $CuCl_2$ (99.9999%), $NiCl_2$ (99.9%), $GaCl_3$ (99.99+%), ZnI_2 (99.99%), $MoCl_5$ (99.99%), H_2PtCl_6 (99.9%), $TeBr_4$ (99%), and $AuCl_3$. The oxide support was neutral activated Al_2O_3 with a specific surface area of 155 m^2/g and 150 mesh size purchased from Aldrich and dried under vacuum at room temperature. Either a 0.25-mm-thick 99.99+% indium foil or a 0.5-mm-thick 99.99% lead foil was used to mount the samples for XPS studies.

The reduction was carried out in an H cell with a medium frit.[31] The cell was evacuated to less than 2×10^{-5} Torr and a small sample (1–600 mg) of the desired metal salt was added to the H cell in a helium-filled glovebox. After removal from the glovebox, the H cell and an ampule of presynthesized alkalide or electride (about 0.5 mmol) which had been kept cold in liquid nitrogen, was transferred to a glovebag that contained a nitrogen atmosphere. The ampule was broken open, and the contents were poured into the other side of the H cell. A liquid nitrogen bath was used to cool the cell to prevent decomposition of the alkalide or electride.

The H cell was once again placed on the vacuum line. It was kept cold by immersion in a bath of liquid nitrogen until the cell had been pumped down to about 10^{-4} Torr, and then in a bath of isopropyl alcohol to which dry ice had been added to keep the temperature at about −50 °C. About 20 mL of prepurified dimethyl ether or tetrahydrofuran was then distilled into each side.

The solvent had been stored under its vapor pressure after pumping out the nitrogen gas to about 10^{-5} Torr (freeze–pump–thaw). Enough blue solution of the alkalide or electride was poured through the frit to react with the solution of the metal salt to be reduced after both solids had been completely dissolved in the solvent.

The alkalides and electrides can also be prepared in situ. For example, 5 mmol of $K^+(15C5)_2K^-$ could be prepared as follows: An H cell was pumped to about 2×10^{-5} Torr and 0.39 g of potassium metal (10 mmol) was added to the H cell in the helium-filled glovebox. After evacuation, the H cell was cooled to about −60 °C and about 10 mL of liquid ammonia was condensed in the H cell to form a blue solution. Then all the ammonia was distilled into a solvent bottle on the vacuum line. After all the ammonia had been removed, a high surface area sample of potassium metal was left inside the H cell, and the H cell was put back into the helium-filled drybox.

An appropriate amount of the desired metal salt was added to the other side of the H cell and about 2.20 g of 15C5 crown ether (10 mmol) was placed into the potassium metal side. The H cell was then removed from the glovebox, evacuated, and kept cold at −50 °C with a cold isopropyl alcohol bath. About 20 mL of prepurified dimethyl ether or tetrahydrofuran was then distilled into each side. The H cell was then placed in dry ice overnight to allow complexation of the potassium metal by 15C5. The reduction reaction was then carried out in a −50 °C isopropyl alcohol bath by pouring the potasside solution through the frit of the H cell into the solution of the metal salt.

The reaction was complete immediately after the addition of alkalide or electride as indicated by fading of the blue color. A slight excess of alkalide or electride was added until the blue color no longer disappeared to make sure that the reaction was complete. Usually, colloidal solutions were initially formed as indicated by the presence of transparent colored solutions that scattered a light beam. After aggregation of particles that required times from a few minutes to a few hours, the solvent was distilled off under vacuum. The products were removed from the walls of the H cell and mounted on indium or lead foil in the helium-filled glovebox. A vacuum transfer vessel, which was designed to transfer chemically reactive specimens from a controlled atmosphere to an analytical system, was used to carry the sample from the glovebox to the X-ray photoelectron spectroscopy (XPS) transfer chamber. The pressure in the main chamber of the XPS instrument was kept below 3×10^{-8} Torr during measurement.

In some cases, deionized and degassed distilled water or prepurified methanol was used to wash away the byproducts. The residue obtained by evaporation of the synthesis solvent was removed from the cell in a nitrogen-filled glovebox and placed into a test tube. About 10 mL of washing solvent was then added to the test tube (still inside the nitrogen-filled glovebag). Washing was performed by centrifugation to separated the undissolved metal particles from the water- or methanol-soluble byproducts. Recently, oxophilic metal samples have been repeatedly washed in the H cell with liquid ammonia, which effectively removes the ionic byproducts without the need to expose the sample to a glovebag atmosphere. Powder X-ray diffraction (XRD) patterns were recorded by placing the precipitate on a glass slide (either with or without washing). A drop of washed suspension was put onto a transmission electron microscope (TEM) carbon-coated grid and allowed to dry in the air, after which TEM micrographs, energy-dispersive spectroscopy (EDS) and selected area electron diffraction (SAD) patterns were made. Obviously, this procedure could only be used with the less reactive metals.

X-ray photoelectron spectroscopy (XPS), which is also commonly termed electron spectroscopy for chemical analysis (ESCA) is one of a number of surface analysis techniques. In addition to its surface sensitivity, XPS is capable of providing chemical information such as the oxidation state and the nature of the chemical bonding, as well as elemental composition. Therefore, it is a preferred method for the characterization of the surface composition of these nanoscale particles. X-ray photoelectron spectroscopy was performed with a Perkin-Elmer PHI 5400 ESCA/XPS spectrometer system. Its analyzer is a spherical capacitor electron energy analyzer (SCA) with an Omni-Focus II lens and a small area lens (200-μm diameter to 3 mm × 10 mm with four selectable apertures). This permits efficient small area analysis without sacrificing overall system analytical flexibility for Auger parameter and photon-dependent depth-profiling studies. Unlike a focused X-ray source, the small spot ESCA design gives an energy resolution that is independent of the analysis area.

The most commonly used anode material for ESCA/XPS is magnesium which has a Kα X-ray energy of 1253.6 eV. It has a narrow natural X-ray line width which facilitates chemical species interpretation and is a highly efficient source of X-rays at moderate power. The system is also equipped with a monochromator to deliver the highest available energy resolution, in which case, Al Kα (1486.6 eV) X-rays are used. All data were recorded by scans at 15 kV. The power of the X-ray sources was 600 W for Al Kα and 400 W for Mg Kα.

XRD patterns provide direct evidence for metal particle formation when the crystallite size is greater than about 3 nm. The width of the strongest XRD line can be used with Scherrer's equation to determine the average size for crystallites with diameters between 3 and 20 nm. A Rigaku D/max-RBX rotating-anode diffractometer equipped with a scintillation counter

(28) Dye, J. L. *Sci. Am.* **1987**, *257*, 66.
(29) Dye, J. L. *J. Phys. Chem.* **1980**, *84*, 1084.
(30) Tsai, K. L.; Dye, J. L. *J. Am. Chem. Soc.* **1991**, *113*, 1650.
(31) "Double Tube" from Kontes, Vineland, NJ 08360.

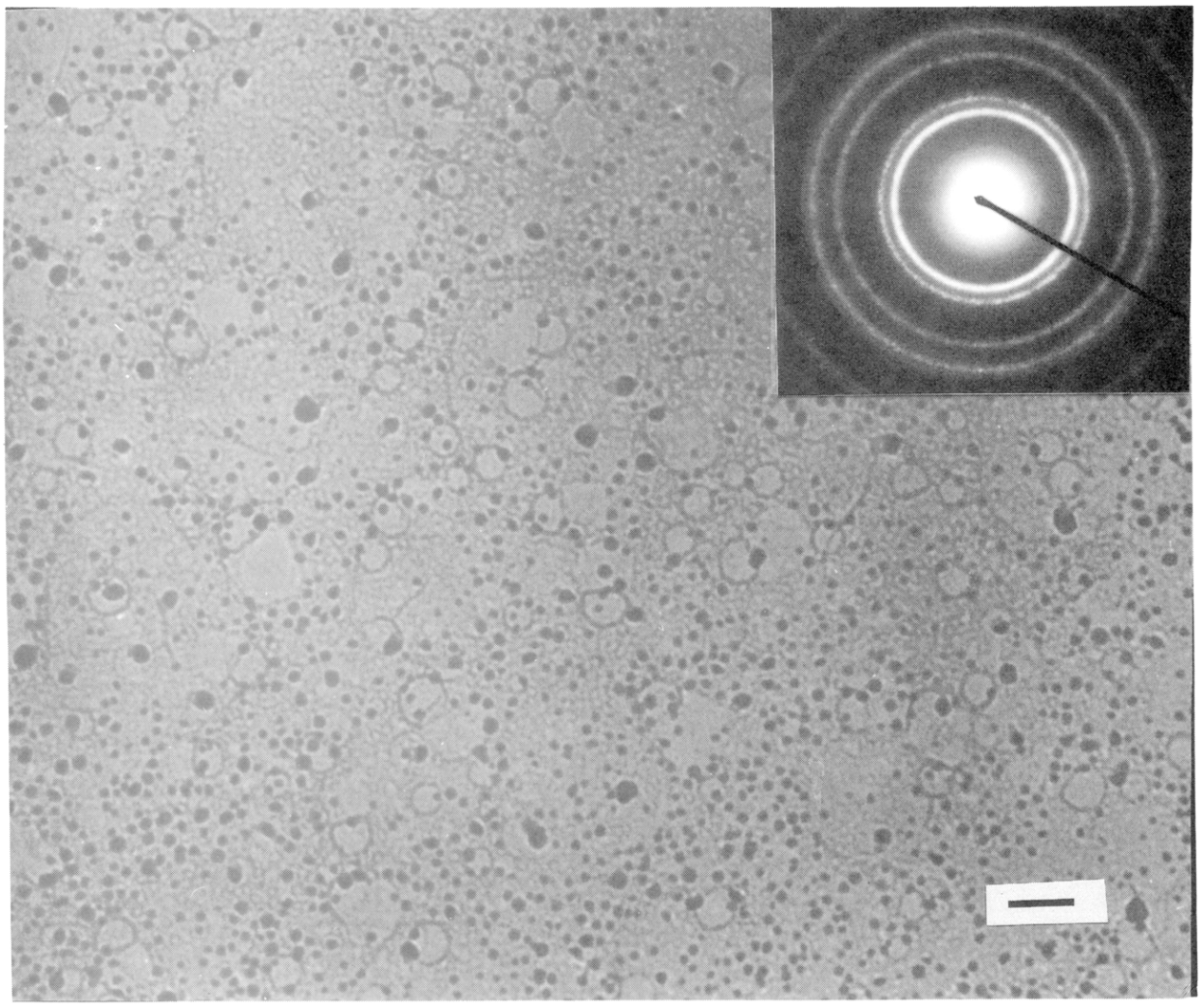

Figure 1. Electron micrograph of Au particles (bar = 330 Å). The SAD pattern in the upper right corner shows the cubic structure of gold.

detector and a graphite monochromator to yield Cu Kα (wavelength 1.541 84 Å) radiation was used under the control of a DEC Microvax computer. All data were recorded by scans at 45 kV and 80 mA.

A JEOL 100 CX II transmission electron microscope operating at 100 kV was used for imaging, EDS, and SAD studies. The images provided information about particle sizes and the morphology of aggregation. A Nicolet 740 FT-IR spectrometer was used to identify the organic compounds on the metal surface.

Results

The procedure for the preparation of small metal particles was described above. While nearly any soluble metallic compound is reduced by alkalides or electrides in Me_2O or THF, the less reactive noble metals, Au, Pt, etc., are easiest to isolate and characterize. Gold was used to test the method and to develop the methodology because $AuCl_3$ is highly soluble in Me_2O and can be easily obtained as the anhydrous compound, and because the product, Au metal, does not oxidize easily when exposed to the air while almost all other metals do when they are in the nanophase state.

Gold. Gold chloride, $AuCl_3$, was reduced by the alkalide, $K^+(15C5)_2K^-$, to produce small metallic gold particles. These were fully characterized by XRD, SAD, and XPS. A typical reduction reaction follows the scheme

$$2AuCl_3 + 3K^+(15C5)_2K^- \rightarrow 2Au + 3K^+(15C5)_2Cl^- + 3KCl$$

or

$$AuCl_3 + 3K^+(15C5)_2e^- \rightarrow Au + 3K^+(15C5)_2Cl^-$$

Only metallic gold peaks were detected by XRD from the precipitates after washing away the byproducts, $K^+(15C5)_2Cl^-$ and KCl, with water or methanol. The micrograph of Figure 1 agrees well with the particle size of about 100 Å as measured by X-ray line broadening of gold produced in the same run. The average diameter could be estimated from Scherrer's equation:[32]

$$L_{hkl} = K\lambda/\beta \cos\theta$$

in which L is the average crystallite size along the direction of the Miller indices (hkl), λ is the wavelength of the X-rays used (e.g., Cu Kα is 1.540 Å), K is Scherrer's constant and has a value of about 0.9, θ is the Bragg angle, and β is the peak width at half-height in radians.

(32) Klug, H. P.; Alexander, L. E. *X-ray Diffraction Procedures for Polycrystalline and Amorphous Materials*; John Wiley & Sons: New York, 1962; pp 491–538.

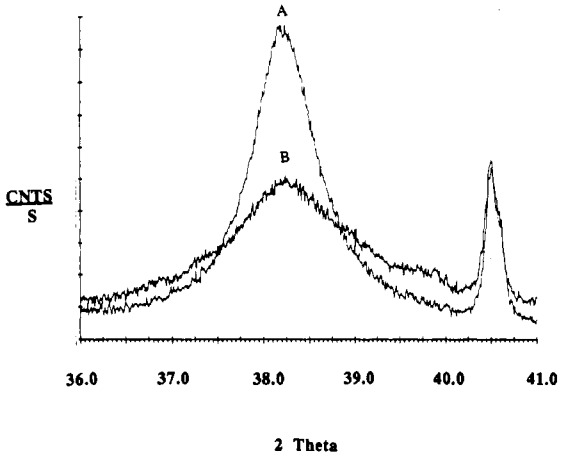

Figure 2. XRD spectra of the products from the reduction of $AuCl_3$ with $K(15C5)_2K$. Solution A with a concentration of 6.5 $\times 10^{-4}$ M of $AuCl_3$ formed 10.5-nm Au particles while solution B with a smaller concentration of 1.6×10^{-4} M yielded a smaller average particle size of 5.8 nm. Note that the byproduct peak width from KCl(220) at 40.56° remains almost the same even when different Au particle sizes formed.

An SAD pattern was also obtained from the same area and is shown at the top of the micrograph. The ring pattern confirms all of the *d* spacings of gold.

In an attempt to modify the particle size, two $AuCl_3$ solutions with different concentrations were reduced with $K^+(15C5)_2K^-$ in Me_2O and the products were collected by distilling out solvent. The XRD data showed that the higher concentration formed larger particles of Au. A 1.6×10^{-4} M $AuCl_3$ solution formed 5.8-nm Au particles while the higher concentration (6.5×10^{-4} M) formed larger Au particles (10.5 nm) as shown in Figure 2. However, the byproduct crystallite sizes remained almost the same even when different Au particle sizes resulted. This was verified by the same peak width from KCl(220) at $2\theta = 40.56°$ as also shown in Figure 2.

A gold colloidal solution always formed first by reaction of the blue solution of alkalide or electride with gold chloride. The colloidal solution disappeared as more and more products were produced. A lot of gray-black mixture of $K^+(15C5)_2Cl^-$, KCl and Au settled to the bottom of the H cell. A colloidal gold solution could be formed again after removal of the reaction solvent by placing the reaction products into water. The aqueous gold colloid was stable for a period of at least several months. The optical absorption spectra of such a gold colloid solution (ruby red) is shown in Figure 3. The 520-nm peak was assigned to surface plasmon absorption as indicated by Abe et al.[33] The same optical peak has also been found for deposited particles (12-nm diameter) in glass.[34]

This method can also be used to prepare highly dispersed metals on oxide surfaces as previously done by other methods.[6,14] To verify this, $AuCl_3$ in Me_2O was adsorbed on neutral activated Al_2O_3 (155 m^2/g) and reduced with $K^+(15C5)_2K^-$ in Me_2O. The Al_2O_3 was evacuated for several days to remove H_2O, but may still have had surface –OH groups that could react with the reducing agent. Au particles (about 6-nm average diameter) were randomly dispersed on the surface as shown in Figure 4. It should be noted that heat treatment and dehydroxylation of the

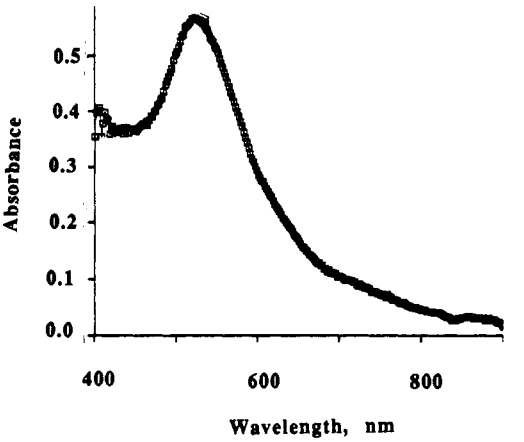

Figure 3. Optical absorption spectra of a ruby-red Au colloidal solution showing a strong surface plasmon absorption peak at 520 nm.

Al_2O_3 might affect the metal particle size and morphology significantly.[35]

By using all of the characterization techniques described above, it was often possible to identify the major phase or phases resulting from reduction and to obtain particle size information. But the high reactivity of nanoscale metal particles and the presence of organic complexants and solvents often resulted in the inclusion of organic decomposition products. FT-IR spectroscopy was used to demonstrate their presence and to identify major IR-active groups on the surface of the metal particles as shown in Figure 5. The sample was prepared by grinding and pressing 5 mg of the washed gold particles mixed with KBr powder. The following peak positions were identified: 457, 540, 786 (C–H or O–H), 951 and 1074 (C–O), 1375 (major impurity from KBr), 1629 (O–H), 2848 and 2916 (C–H), and 3437 (O–H). Analysis of a sample of washed Au particles showed atomic percentages of 0.70% for carbon, <0.5% for hydrogen (Galbraith Laboratories, Inc.).

(II) Tellurium. $TeBr_4$ was reduced by $K^+(15C5)_2e^-$ in dimethyl ether. Figure 6A shows the XPS $3d_{5/2}$ binding energy at 573.0 eV of elemental Te before washing. After oxidizing these products in air for 3 min, the oxide XPS $3d_{5/2}$ peak at 576.3 eV was larger than the metal peaks as shown in Figure 6B. As shown in Figure 6C, elemental Te peaks as well as oxide peaks were observed after washing the original reduction product with methanol.

Only elemental Te peaks were observed by powder X-ray diffraction as shown in Figure 7A. The average particle size estimated from line broadening is 117 Å, and the micrograph (Figure 7B) shows the presence of rodlike shapes. The electron diffraction pattern confirms the hexagonal structure of elemental Te with $a = 4.46$ Å and $c = 5.93$ Å.

(III) Copper. Although bulk copper is very stable in air, it can be oxidized at room temperature when the particles are of nanometer size. $CuCl_2$ was reduced in Me_2O by the present method to produce small metallic copper particles. These were fully characterized by X-ray powder diffraction, electron diffraction, and X-ray photoelectron spectroscopy. Only metallic copper peaks were detected by XRD from the precipitates after washing away the byproducts. The mean particle size as obtained from

(33) Abe, H.; Charle, K. P.; Tesche, B.; Schulze, W. *J. Chem. Phys.* **1982**, *68*, 137.
(34) Doremus, R. H. *J. Chem. Phys.* **1964**, *40*, 2389.
(35) Tan, B. J.; Klabuunde, K. J.; Sherwood, P. M. A. *J. Am. Chem. Soc.* **1991**, *113*, 855.

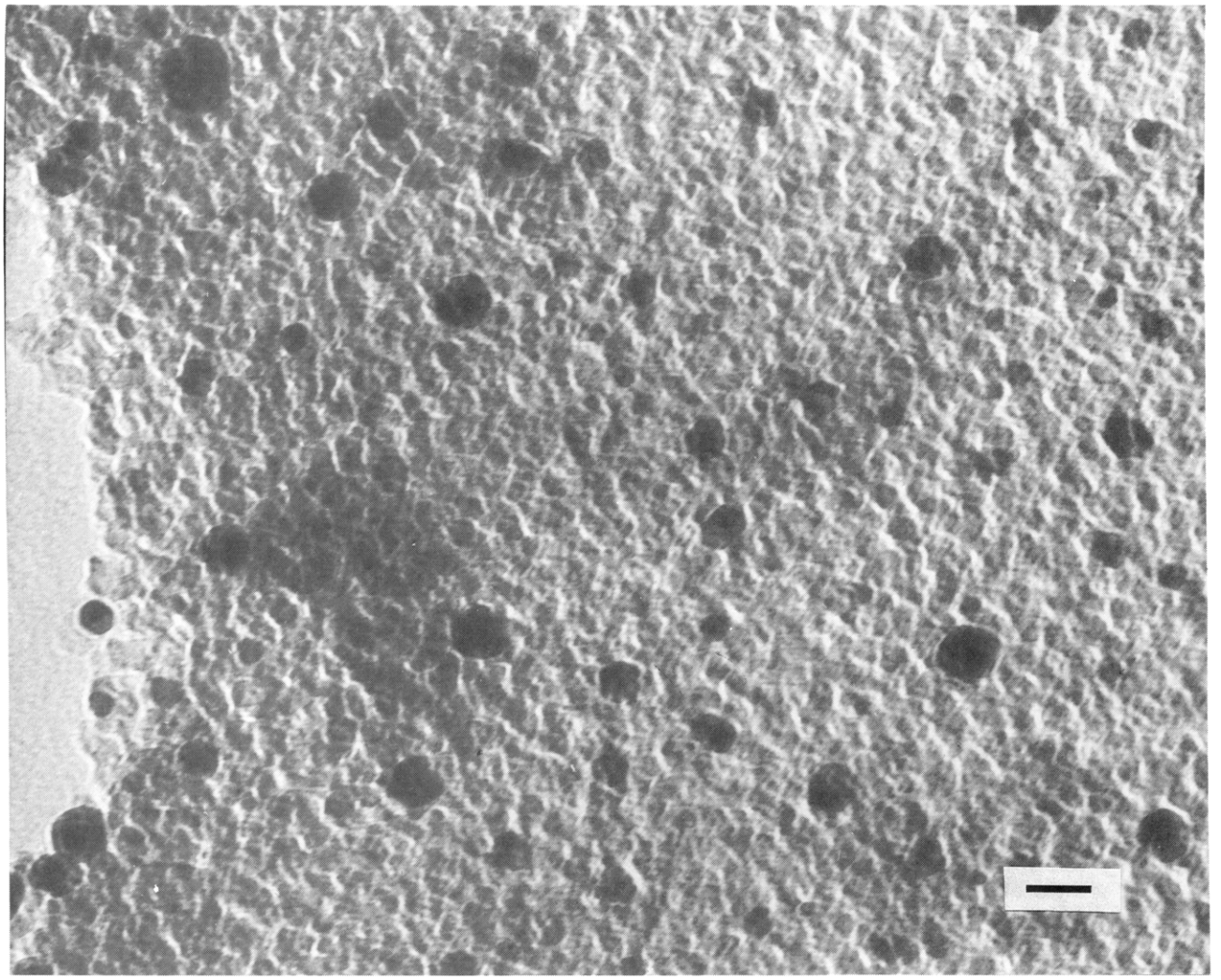

Figure 4. Electron micrograph of Au particles on Al_2O_3 (bar = 180 Å).

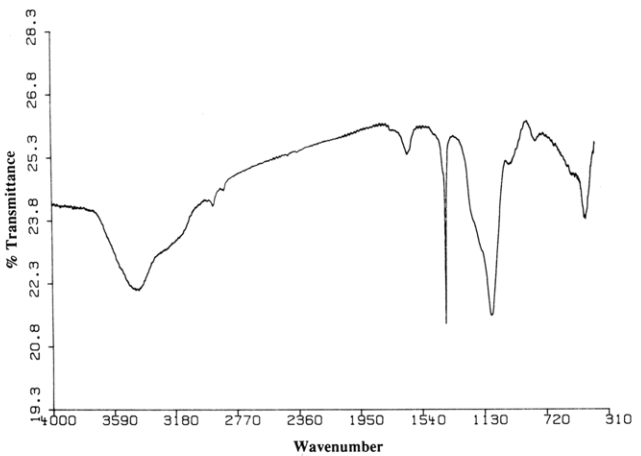

Figure 5. FT-IR spectra of washed Au particles. The peak assignments are given in the text.

the XRD line broadening of the strongest peak of Cu(111) was about 57 Å after washing with methanol. An electron micrograph agrees well with the average particle size of 57 Å obtained from the XRD line broadening of the metallic Cu product from the same run (see Figure 2 of ref 36) SAD showed the characteristic electron diffraction pattern of metallic copper. These particles were also characterized by energy dispersive spectroscopy which showed only Cu peaks on the Ni grid.

The small Cu particles were also characterized by XPS and only the $2p_{3/2}$ peak with a binding energy of 932.6 eV and the $2p_{1/2}$ line at 952.4 eV appear before washing and after washing away the byproducts with methanol. The XPS studies showed that some CuO was present on the Cu surface after exposing the sample to air for 24 h.

(IV) Nickel. By adding triethylphosphine to increase its solubility, $NiBr_2$ was reduced by $K^+(15C5)_2K^-$ in dimethyl ether. The products were kept in the H cell under vacuum for 4 days and analyzed by XPS which showed only the metallic Ni $2p_{3/2}$ peak with a binding energy of 852.6 eV. Small NiO shakeup peaks appeared when these particles were oxidized in air for 24 h, and all Ni particles were oxidized when the initial reduction products were exposed to a glovebag atmosphere and washed with methanol.

(V) Antimony. $SbCl_5$ was reduced by $K^+(15C5)_2K^-$ in dimethyl ether. Both metallic and oxide $3d_{5/2}$ XPS peaks appear, with binding energies of 528.0 and 530.4 eV as shown in Figure 8A,B before and after washing with methanol. Note that the O 1s peak at 532.4 eV from the crown ether disappeared upon washing. The washed products were sputtered by an argon ion beam for 20 min. The result, shown in Figure 8C, indicates that only a small amount of oxide was left after sputtering.

(36) Dye, J. L.; Tsai, K. L. *Faraday Discuss. Chem. Soc.* **1991**, *92*, 45.

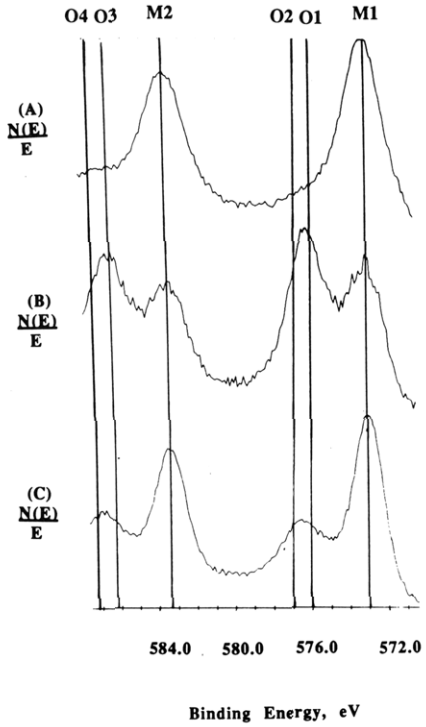

Figure 6. XPS spectrum of Te. (A) Very clean elemental tellurium peaks after reduction but without exposure to air. (B) Both metallic Te and Te oxides on the surface after exposing the products to air for 3 min. (C) Small amount of Te oxide on metallic Te after washing away byproducts with methanol. Note the following peak assignments: M1 → metallic Te $3d_{5/2}$, M2 → metallic Te $3d_{3/2}$, O1 → TeO $3d_{5/2}$, O2 → TeO_2 $3d_{5/2}$, O3 → TeO $3d_{3/2}$, O4 → TeO_2 $3d_{3/2}$.

(VI) Gallium. $GaCl_3$ was reduced by $K^+(15C5)_2K^-$ in dimethyl ether. Both metallic and oxide $L_3M_{45}M_{45}$ Auger peaks with kinetic energies of 1067.9 and 1062.5 eV, respectively, were observed for an unwashed sample. The sample was bombarded by argon ions for 2 and 5 min with progressively greater relative intensity of the metal peak.

(VII) Zinc. ZnI_2 was reduced by $K^+(15C5)_2K^-$ in dimethyl ether. Both metallic and oxide $L_3M_{45}M_{45}$ Auger peaks were observed with kinetic energies of 991.8 and 987.2 eV, respectively. The sample was bombarded by argon ions for 2 and 4 min with a progressive increase in the relative intensity of the metal peaks.

(VIII) Molybdenum. $MoCl_5$ was reduced by K^+-$(15C5)_2K^-$ in dimethyl ether. Both metallic and oxide $3d_{5/2}$ XPS peaks appeared with binding energies of 230.0 and 234.3 eV, respectively. The sample was bombarded by argon ions for 10 and 30 min with increasing relative intensity of the metal peak. The oxide on molybdenum appears to be harder to remove than that on either zinc or gallium so that it took a longer time to sputter off the oxide.

(IX) Tin. $SnCl_4$ was reduced by $K^+(15C5)_2K^-$ in dimethyl ether. Both metallic and oxide $3d_{5/2}$ XPS peaks appeared with binding energies of 485.2 and 487.0 eV, respectively. The sample was exposed to the air for 30 s, after which the intensity of the metallic peaks decreased by about a factor of 2.

(X) Platinum. H_2PtCl_6 (hydrated) was reduced by $K^+(15C5)_2K^-$ in THF. The metallic Pt particles were characterized by XPS and only the $4f_{7/2}$ peak with binding energy of 71.1 eV and the $4f_{5/2}$ peak at 74.5 eV appear after washing away the byproducts with methanol. The

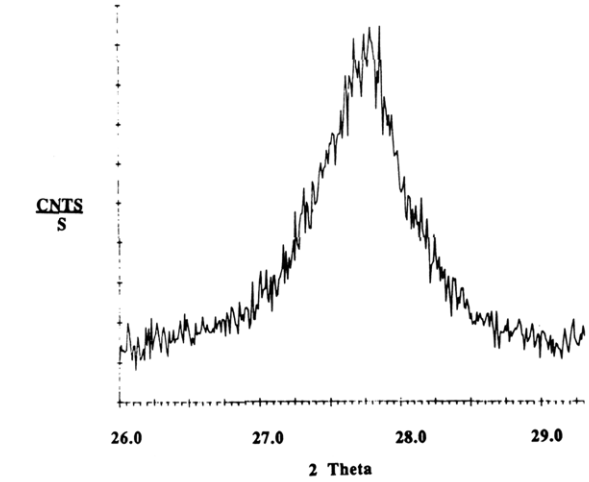

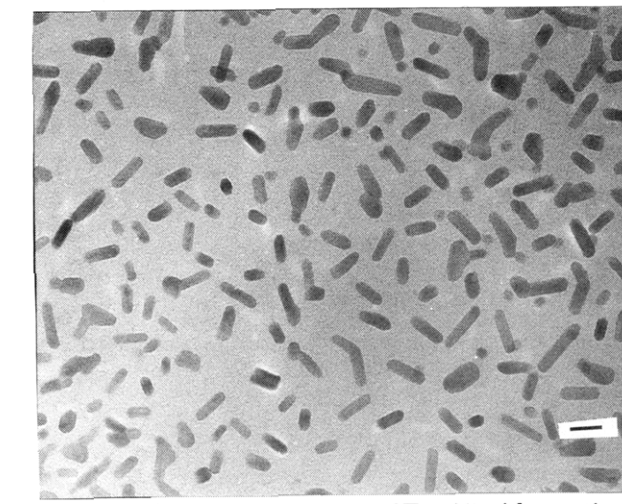

Figure 7. (A, top) XRD spectrum of Te(101) with an estimated average particle size of 120 Å. (B, bottom) Electron micrograph of Te particles that shows the rodlike shape of the particles (bar = 230 Å).

TEM micrograph shows an average particle size of about 4 nm. An SAD pattern also showed only elemental platinum.

(XI) Titanium. $TiCl_4$ was reduced by $K^+(15C5)_2K^-$ in dimethyl ether. However, by the time the product was transferred to the XPS instrument, no metal could be observed either with or without washing, although initial reduction had occurred as indicated by the fading of the blue color of the alkalide solution. After solvent removal, only titanium oxide could be identified. Whether this occurred by reaction of titanium metal with the complexant or solvent or by subsequent oxidation is not known.

Discussion

All soluble metal compounds tested to date are reduced by K^- or e^- in Me_2O or THF at −50 °C immediately upon mixing. The presence of a stable blue color after the addition of excess reductant indicates that the reduction is complete and that we are not merely catalytically decomposing the alkali metal solution. All but $TiCl_4$ were shown by XPS and/or XPD and SAD methods to contain metal particles after solvent removal. Some could be washed with outgassed methanol without significant oxidation. Argon ion sputtering to remove surface layers indicated that those particles with both oxide and metal XPS peaks contained metal beneath an oxide layer. While

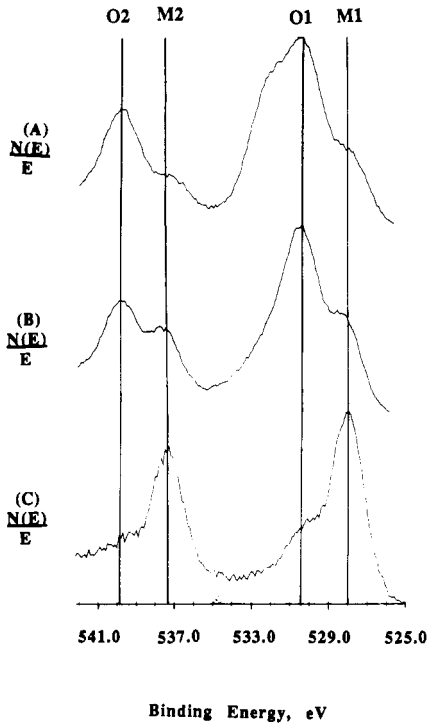

Figure 8. XPS spectrum of Sb. (A) Both elemental antimony and antimony oxides on the surface after reduction. Note that there is a shoulder at O1 due to the oxygen 1s peak from the crown ether. (B) No oxygen 1s shoulder because the crown ether was washed away with methanol. (C) Oxide can be sputtered away by argon ions. Note the following peak assignments: M1 → metallic Sb $3d_{5/2}$, M2 → metallic Sb $3d_{3/2}$, O1 → $Sb_2O_5 3d_{5/2}$, O2 → Sb_2O_5 $3d_{3/2}$.

oxide reduction by the argon beam cannot be excluded in all cases, it has been shown[37] that at least ZnO and SnO_2 are not reduced by argon ion bombardment.

In most cases, the average crystallite diameters were less than 3 nm as indicated by the absence of XRD peaks of the metal. For Au, Cu, and Te, however, the particles were large enough to determine their average diameter by XRD, and the results were in excellent agreement with the size distributions obtained from electron micrographs. The average size of gold particles was smaller when more dilute solutions of $AuCl_3$ were reduced. However, higher concentrations of $AuCl_3$ might not necessarily lead to larger particles. For example, when $AuCl_3$ is reduced in aqueous solution smaller particles are formed at higher concentrations.[38] By contrast, however solvated Au atoms behave as seen in this work, in that higher concentrations lead to larger particles. In most cases with all metals, a colloidal suspension is first produced as indicated by light scattering and color, followed by slow aggregation of the colloid to a precipitate that can be separated by centrifugation. To carry out centrifugation, however, the samples had to be exposed to a glovebag atmosphere, which probably resulted in some oxidation except for the noble metals.

A major advantage of this method for producing metallic colloids in nonaqueous solvents and nanoscale metal particles is that the reactions occur rapidly with homogeneous solutions. This has permitted formation of intermetallic compounds or alloys when two metal salts are reduced simultaneously.[36] The strong reducing power (~−3 V) of alkalides and electrides means that practically any soluble metal salt can be reduced to the metallic state. The more oxophilic metals, however, are so reactive that it is difficult to separate them from the solvent and the byproducts without some oxidation.

While the noble metals and some others such as Cu and Te can be separated from the byproducts, K^+X^- and $K^+(15C5)_2X^-$ (X = Cl, Br, and I), by washing with methanol, more oxophilic metals were oxidized by this procedure. We have had some success in removing the byproducts with liquid ammonia without metal oxidation, but the low solubility of KCl in ammonia requires multiple washings. Other anions such as Br^- may improve the ability to wash away the byproducts. It should be noted that the crown ether, 15-crown-5, can be recovered quantitatively for reuse if desired. Thus the net reaction is the reduction of a metal salt with potassium.

The reactive nature of nanoscale metals and the high surface are a lead to the inclusion of organic residues on the surface. We have been able in some cases to remove most of the organic contaminants by heating the samples to 100–150 °C under vacuum. Such procedures, coupled with other washing solvents should improve the purity. With very oxophilic metals it might not be possible to prevent oxidation by reaction with the complexant or solvent. So far, however, only Ti has failed to yield metal although some other metals have oxide on the surface. Since nanoscale metal particles are very reactive, this method of producing highly active metal powders might prove useful in organometallic synthesis.

Acknowledgment. This work was supported by the U.S. National Science Foundation under Solid-State Chemistry Grant No. DMR 90-17292 and by the Michigan State University Center for Fundamental Materials Research. We thank the Center for Electron Optics and the Composite Materials and Structure Center at Michigan State University for the used of TEM and XPS instrumentation. The help of Mr. David E. Olszewski in the study of the effect of dilution on gold particle size is gratefully acknowledged. We also thank Mr. Xian-Zhong Chen for helping with the ammonia washing development.

(37) Kim, K. S., Baitinger, W. E., Amy, J. W.; Winograd, N. *J. Electron. Spectrosc.* **1974**, *5*, 351.
(38) Turkevich, J.; Hillier, J. *J. Phys. Chem.* **1953**, *57*, 670 and references therein.